High confinement suspended micro-ring resonators in silicon-on-insulator

Linnell Martinez and Michal Lipson

Department of Electrical and Computer Engineering, Cornell University, Ithaca, New York 14850
lm262@cornell.edu, lipson@ece.cornell.edu

http://nanophotonics.ece.cornell.edu

Abstract: We demonstrate suspended micrometer-scale ring resonators with quality factors exceeding 15,000. The high quality factor is achieved by using a suspension method where the disturbance of the optical mode due to the support arms is minimized. We show an insertion loss of less than .02dB per suspension bridge.

OCIS codes: (230.5750) Resonators; (230.0230) Optical devices

References and links

1. Y. Akahane, T. Asano, B.-S. Song, and S. Noda, "High-Q photonic nanocavity in a two-dimensional photonic crystal," Nature **425,** 944-947 (2003).
2. T. Baba and D. Sano, "Low-threshold lasing and Purcell effect in microdisk lasers at room temperature," IEEE J. Sel. Top. Quantum. **9,** 1340-1346 (2003).
3. T. J. Kippenberg, S. M. Spillane, and K. J. Vahala," Kerr-nonlinearity optical parametric oscillation in an ultrahigh-Q toroid microcavity," Phys. Rev. Lett. **93,** 083904-1 (2004).
4. O. Painter, R. K. Lee, A. Scherer, A. Yariv, J. D. O'Brien, P. D. Dapkus, and I. Kim, "Two-dimensional photonic band-gap defect mode laser," Science **284,** 1819-1821 (1999).
5. Q. Xu, V. R. Almeida, and M. Lipson, "Demonstration of high Raman gain in a submicrometer-size silicon-on-insulator waveguide," Opt. Lett. **30,** 35-37 (2005).
6. A. Yariv, "Universal relations for coupling of optical power between microresonators and dielectric waveguides," Electron. Lett. **36,** 321-322 (2000).
7. V. R. Almeida, C. A. Barrios, R. R. Panepucci, and M. Lipson, "All-optical control of light on a silicon chip," Nature **431,** 1081-1084 (2004).
8. T. J. Kippenberg, S. M. Spillane, and K. J. Vahala, "Demonstration of ultra-high-Q small mode volume toroid microcavities on a chip," Appl. Phys. Lett. **85,** 6113-6115 (2004).
9. B. Matthew, S. Kartik, E. B. Paul, and P. Oskar, "Rayleigh scattering, mode coupling, and optical loss in silicon microdisks," Appl. Phys. Lett. **85,** 3693-3695 (2004).
10. V. R. Almeida, C. A. Barrios, R. R. Panepucci, M. Lipson, M. A. Foster, D. G. Ouzonnov, and A. L. Gaeta, "All-optical switching on a silicon chip," Opt. Lett. **29,** 2867-2869 (2004).
11. T. Baehr-Jones, M. Hochberg, C. Walker, and A. Scherer, "High-Q ring resonators in thin silicon-on-insulator," Appl. Phys. Lett. **85,** 3346-3347 (2004).
12. B.E. Little, S.T. Chu, H.A. Haus, J. Foresi, and J.P. Laine, "Microring resonator channel dropping filters," J. Lightwave Technol. **15,** 998-1005 (1997).
13. B. E. Little, J. S. Foresi, G. Steinmeyer, E. R. Thoen, S. T. Chu, H. A. Haus, E. P. Ippen, L. C. Kimerling, and W. Greene, "Ultra-compact Si-SiO_2 microring resonator optical channel dropping filters," IEEE Photon. Tech. L. **10,** 549-551 (1998).
14. T. Fukazawa, T. Hirano, F. Ohno, and T. Baba, "Low loss intersection of Si photonic wire waveguides," Jpn. J. Appl. Phys. 1 **43,** 646-647 (2004).
15. P. Rabiei, W. H. Steier, Z. Cheng, and L. R. Dalton, "Polymer micro-ring filters and modulators," J. Lightwave Technol., **20,** 1968-1975 (2002).

1. Introduction

Optical micro and nano scale resonant cavities have received much attention recently due to the enhanced light-matter interaction within these systems. Enhanced spontaneous emission (Purcell effect), strong coupling, two photon absorption, and Raman scattering are a few

#70632 - $15.00 USD Received 5 May 2006; revised 8 June 2006; accepted 10 June 2006

examples of phenomena which can be greatly enhanced in a high Q optical resonant cavity [1-6]. The size of the cavities for on-chip applications can be greatly decreased in a high index contrast system due to increase in mode confinement [7]. Recently, in order to benefit from the high index contrast between silicon and air, suspended disk resonators have been demonstrated [8, 9]. In these works the disk is suspended by a post beneath its center and the whispering gallery modes (WGM) propagate in the boundaries of the disks. Because of the low overlap between the optical mode and suspension mechanism, radiation losses are not inherent to these devices and therefore very high Q's can be achieved; however, the limitation of these disks lies in their multi-mode nature, and therefore low degree of confinement.

Rings resonators have a much higher degree of confinement due to their single mode nature. Several rings resonators have been demonstrated in Si/SiO_2 platforms [10-12] with radii as small as 3μm [13]; however, suspended ring resonators have not yet been demonstrated. The difficulty in demonstrating suspended high Q ring resonators is due to the high overlap of the small mode with the suspended arms, which introduce reflections and radiation losses in the system.

2. Analysis of suspension mechanism

The difficulty in achieving high confinement suspended ring resonators lies in the suspended mechanism itself. When suspension arms are used to support the waveguide bridge, the tightly confined mode experiences a large index change in that region. This change in effective index is responsible for the reflections and radiations losses which essentially destroys the Q of the device.

In order to minimize the losses due to the suspended arms, we expand the waveguide so that the overlap between waveguide mode and suspension mechanism is minimal [14]; we use a gradual s-bend profile for the increase in the waveguide geometry, so that reflections at the ring-bridge boundary are minimized. The optimal dimensions of the s-bend bridge were chosen based on those presented in [14] for the elliptical bridge, but with minor changes in length (L_B) and width (W_B) due to our s-bend geometry. The width (W_A) of the suspension arms was also decreased to further reduce mode distortion. By using an s-bend bridge, the mode experiences an adiabatically increase in effective index. Midway through the bridge, where the effective index is at a maximum, the suspension arms have a negligible effect on the already delocalized mode.

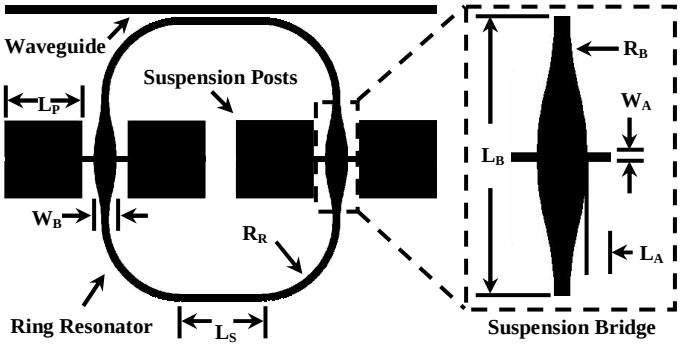

Fig. 1. Layout of suspended ring resonator with corresponding dimensions L_A=0.8μm, L_B,R_B=8μm, L_P,L_S,R_R=5μm, W_A=0.2μm, and W_B=1.4μm

3D FDTD simulations were used to calculate the transmission characteristics of a waveguide bridge as well as the s-bend bridge proposed in this work. The device has been designed to operate for TE-like polarized light and thus all the simulations were performed for TE-like polarization. Indices used in the simulations were 3.46 and 1.0 for Si and air, respectively. In Fig. 2 we show the electric field profile of 1.55μm light for the wave guiding structure under

#70632 - $15.00 USD Received 5 May 2006; revised 8 June 2006; accepted 10 June 2006

study. From this profile we calculate that approximately 93% of the light is confined in the waveguide.

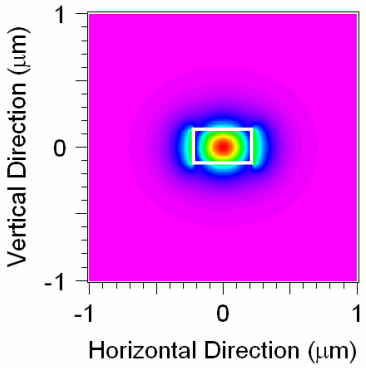

Fig. 2. Optical mode profile of waveguide for TE-like polarized light at 1.55μm

The suspension mechanism strongly impacts the losses per pass of the device. The distributed loss term is given by:

$$\alpha_{eff} L = \alpha_{scat}(2L_S + 2\pi R_R) - 2\ln(T_B) - \ln(1 - |\kappa|^2) \quad (1)$$

where α_{scat}, L_S, R_R, T_B, and κ are the losses due to scattering in the straight and curved sections of the ring resonator, length of straight sections, bend radius, bridge transmission, curved-straight section junction transmission, and coupling coefficient. In order to obtain an estimate for the distributed loss term, we simulated the s-bend bridge as well as the coupling section, and obtained a transmission T_B of 0.995 (losses of 0.02dB per bridge) for the s-bend bridge and 0.965 for a bridge with no s-bend (losses of 0.15dB per bridge). We calculated a coupling coefficient κ of 0.038 and assumed a α_{scat} = 5dB/cm. One can see from (1) that in the case of the waveguide bridge, T_B dominates over all other loss mechanisms.

3. Device fabrication

The device was fabricated using a fairly common patterning and undercutting method. FOX-12, a negative e-beam resist was used to coat a Silicon-on-Insulator (SOI) wafer with a 250nm top Si layer and a 1μm Buried Oxide (BOX) layer. The desired pattern was written using a JEOL 9300 e-beam system and then etched in a PT770 Inductively Coupled Plasma (ICP) etcher. A 1μm SiO_2 cladding was deposited using a plasma-enhanced chemical-vapor deposition (PECVD). We then selectively etch a 30μm^2 area above the device by reactive ion etching (RIE) in an Oxford PlasmaLab 80 system to remove approximately 500nm of the SiO_2 cladding. The coupling waveguide will be suspended over this 30μm length, but note that due to a non-uniform oxide cladding, the waveguide tends to be suspended over a 40-50μm length. The non-uniform oxide layer causes the buffered oxide solution, used in the under-etch step of the release process, to propagate along the corners of the waveguide and therefore suspend a longer region of it. This effect is shown in Fig. 3(a). Waveguide lengths of up to 60μm have been suspended with no noticeable sagging.

#70632 - $15.00 USD Received 5 May 2006; revised 8 June 2006; accepted 10 June 2006

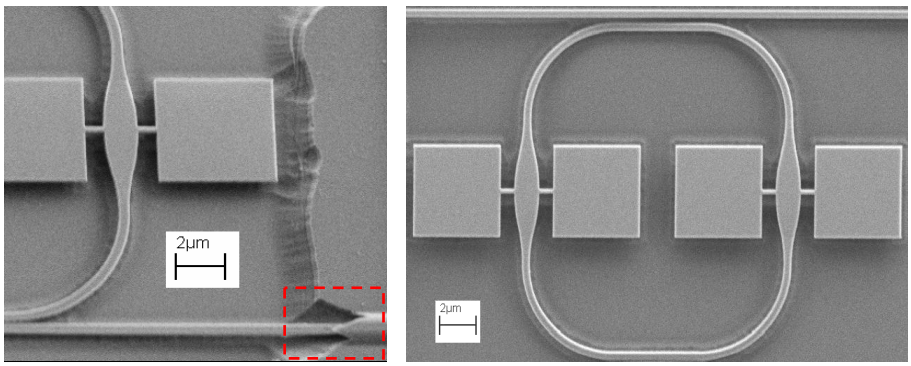

Fig. 3. (a) SEM image showing the effect caused by non-conformal oxide cladding. (b) SEM image showing a fully fabricated device

Following the polishing of the dies, the dies are placed in a 6:1 buffered oxide etch (BOE) solution for approximately ten minutes in order to release the devices. The release process removes approximately 700nm of oxide below the waveguide. This gap is necessary to avoid losses due to coupling of the optical mode to the substrate. The devices are then transferred to a critical point dryer (CPD) to prevent damage from surface tension. Fig. 3(b) shows an SEM of the fabricated device.

4. Experimental results

To characterize the resonator, we couple TE-like polarized light into the input port and measure the response at the output port. All measurements were carried out in an ambient atmosphere. Figure 4(a) shows the transmission spectra of three devices with slightly different ring dimensions. The measured free spectral range (FSR) of approximately 10nm agrees closely with the theoretical value [15] of 9.8nm given by:

$$FSR \approx \frac{\lambda_0^2}{n_g(\lambda)L} \tag{2}$$

where n_g is the group index.

One can clearly see that the resonators exhibit strong spectral features. The resonance for the measured Q of approximately 15,000 is shown in Fig. 4(b).

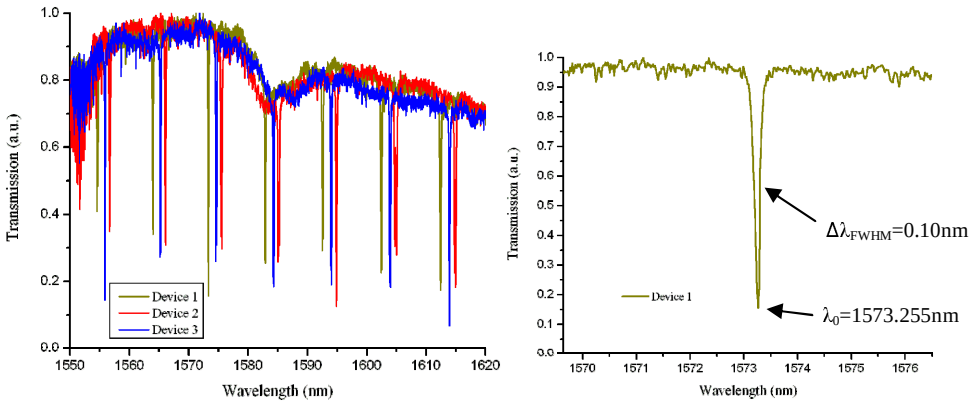

Fig. 4. (a) Output spectra for three different fabricated devices. (b) Resonance showing a Q of approximately 15,000.

#70632 - $15.00 USD
Received 5 May 2006; revised 8 June 2006; accepted 10 June 2006

5. Conclusions

We show for the first time, suspended silicon ring resonators in an SOI platform. A novel suspension method was developed in order to minimize losses created by abrupt changes in effective refractive, thus allowing us to achieve losses of less than .02dB per bridge. These devices due to their high confinement in both planar and transverse direction, offer opportunities in applications requiring highly integrated active devices such as optical filter elements, modulators and all optical switches on silicon.

Acknowledgments

This work was supported by the Science and Technology Centers program of the national Science Foundation (NSF) under agreement DMR-0120967, the Cornell Center for Nanoscale Systems, the Cornell Center for Material Research, and the National Science Foundation's CAREER Grant No. 0446571. The authors would also like to thank Gernot Pomrenke from the Air Force Office of Scientific Research for supporting the work under Grants No. F49620-03-1-0424 and No. FA9550-05-C-0102.

#70632 - $15.00 USD Received 5 May 2006; revised 8 June 2006; accepted 10 June 2006